

# Multi-pass Hot Rolling of Steels

Multi-pass hot rolling is a general practice in the production of plates. An illustration of a plate mill, Fig. 1, is shown below to demonstrate how a series of processes are carried out to produce plates from steel slabs. Slabs are first reheated in a furnace, which reduces its deformation strength sufficiently to allow it to be rolled. High pressure water sprays are then used to remove the oxide layer (scale) built up during prior processes and reheating. Plate rolling mills are mostly of the reversing type, i.e. reducing the gap and hence the stock thickness pass by pass. Once the required dimensions are reached, the plate undergoes an accelerated cooling process where transformations are controlled to obtain the desired microstructure. Finishing procedures are followed which include plate shearing, levelling, and inspection.

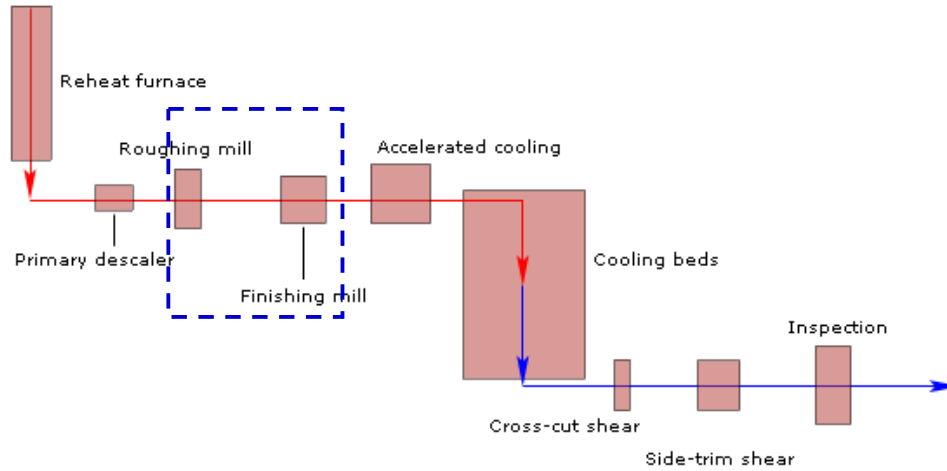


Fig. 1, General description of plate rolling mill.

This note is focused on our recent model development which calculates the evolution of microstructure and rolling forces during multi-pass hot rolling of steels (inside the dotted blue square in Fig. 1). The possible phenomena taking place during hot rolling include: precipitation of MX type carbides or carbonitrides, recrystallisation and grain refinement, and phase transformations, and they interact with each other. Material models have been developed in previous research for deformation-induced-precipitation kinetics [1], recrystallization kinetics and grain refinement [2,3], and phase transformation kinetics [4]. All these models have been incorporated in the current model, which considers the following interactions:

- Interactions between precipitation kinetics and recrystallisation.
- Effect of recrystallisation and precipitation on grain refinement.
- Effect of grain refinement on phase transformation kinetics.
- Effect of recrystallisation, grain refinement and phase transformations on rolling force.

Figs. 2 to 5 demonstrate the evolution of precipitate size and fraction, recrystallisation fraction, grain size, and austenite decomposition, respectively. The experimental data in these figures were taken from Ref. 3 where multi-pass torsion tests were carried out to simulate hot rolling. The chemical composition of the steel is, in wt.%, Fe-0.1C-0.31Si-1.42Mn-0.0053N-0.035Nb. Before torsion tests, specimens were reheated at either 1400°C or 1200°C, which produced a prior austenite grain size of 806 and 129  $\mu\text{m}$ , respectively. Torsion tests consists of 17 passes from 1180 to 700°C at 30°C interval. The interpass time is 30 seconds, giving an equivalent cooling rate of 1 °C/s. The strain rate is fixed at 1.0 s<sup>-1</sup> in all tests, whereas the strain per pass varies from 0.1 to 0.4. Fig. 2 shows the evolution of M(C,N) precipitation at grain boundary (GB) and inside matrix at strain per pass 0.3 after reheating at 1200°C. The fluctuation around 1050°C in Fig. 2(b) is due to the continuous population of new nuclei before reaching site saturation, as a result of which the average precipitate size goes up and down. This happens at a region where precipitate amount is tiny, Fig. 2(a), and therefore is of no practical significance. The calculated recrystallisation fraction, Fig. 3, shows good agreement with experimental data in the austenite region (10000/T < 9.3) but deviates when ferrite starts to form, Fig. 5. It can be seen in Fig. 4 that the grain size calculations are in good agreement with the

experimental values for both reheating conditions. It is also observed that, in spite of the big difference in the prior austenite grain size, the grain sizes start to converge after several passes. When temperature goes below  $A_3$  temperature of the steel (calculated as  $834^\circ\text{C}$ ), austenite decomposition takes place and phases that may form are ferrite, pearlite, bainite and martensite [4]. In the temperature region of deformation ( $1180$  to  $700^\circ\text{C}$ ) at cooling rate  $1^\circ\text{C/s}$ , ferrite is the only phase formed, Fig. 5. If further cooling to room temperature is assumed to be at the same rate, martensite will start to form at around  $400^\circ\text{C}$ .

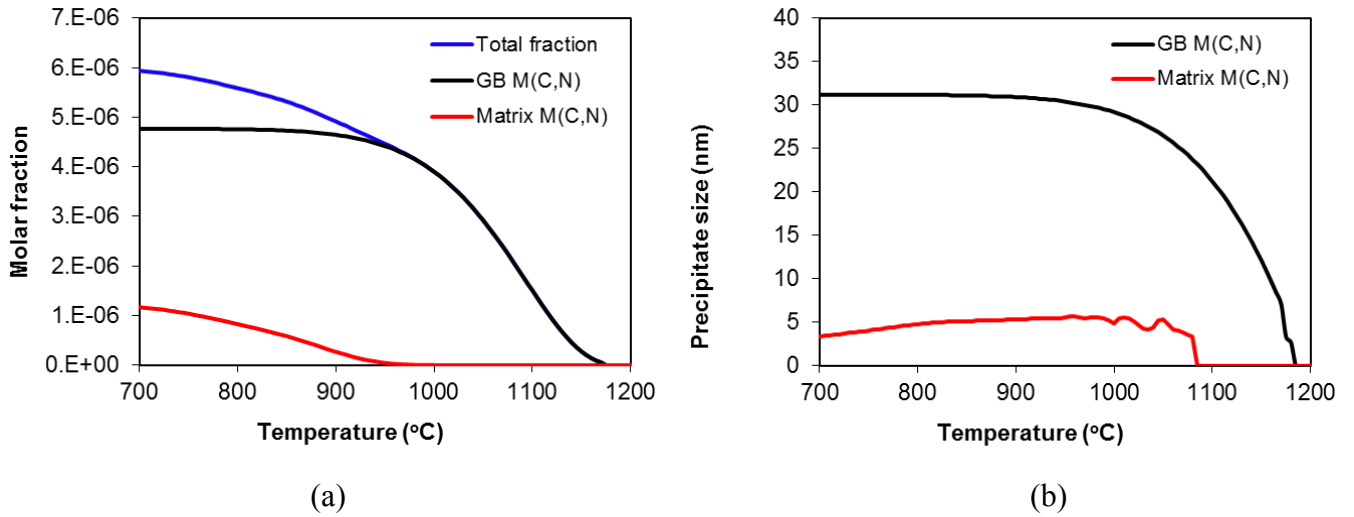


Fig. 2, Evolution of M(C,N) precipitation at grain boundary (GB) and inside matrix at strain per pass 0.3 after reheating at  $1200^\circ\text{C}$ , (a) precipitate amount, and (b) precipitate size.

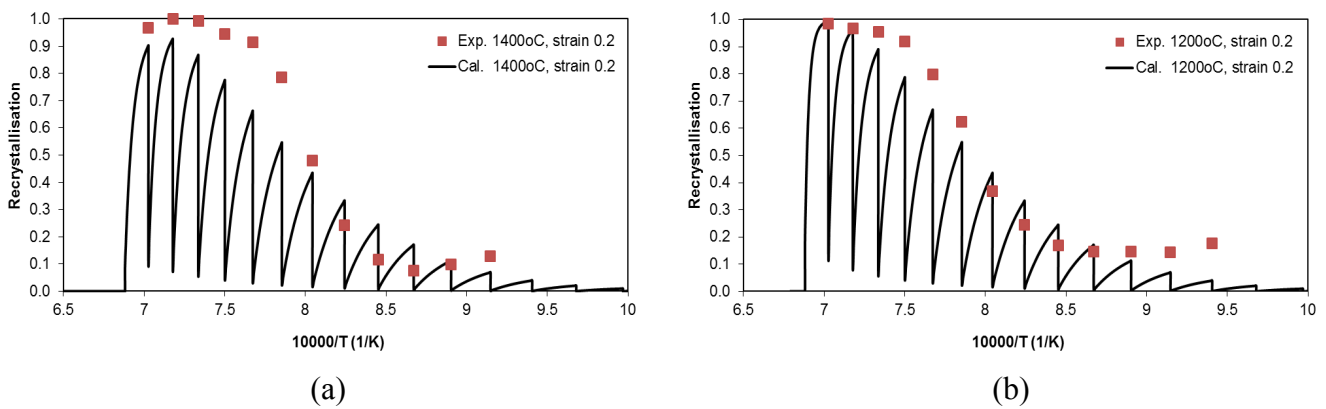


Fig. 3, Evolution of recrystallisation fraction during deformation at strain per pass 0.2 after reheating at different temperatures, (a)  $1400^\circ\text{C}$ , and (b)  $1200^\circ\text{C}$ .

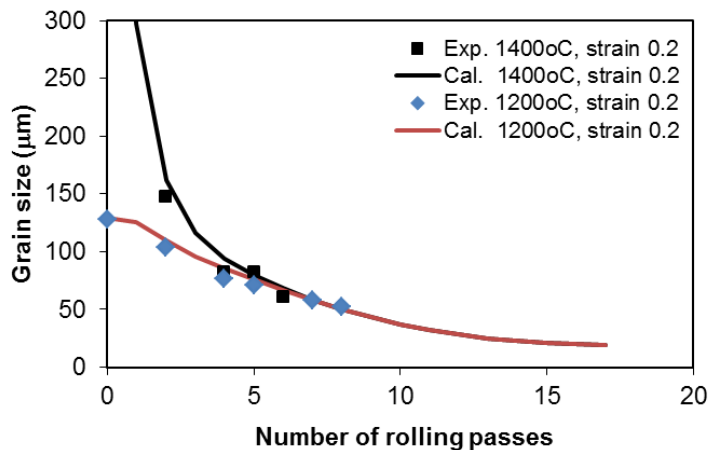


Fig. 4, Evolution of grain size after reheating at  $1400^\circ\text{C}$  and  $1200^\circ\text{C}$ , prior austenite grain size as  $806$  and  $129 \mu\text{m}$ , respectively.

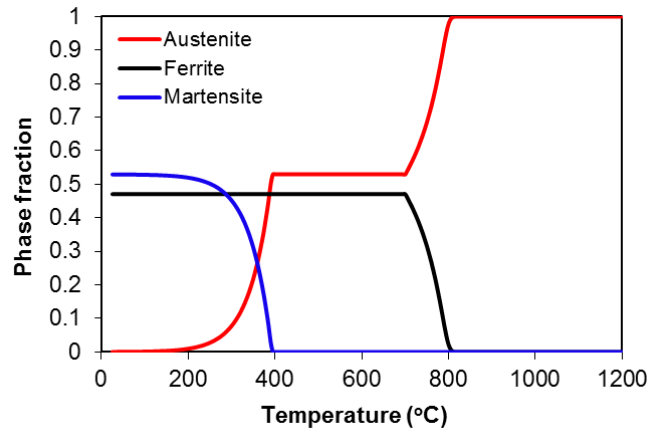


Fig. 5, Evolution of austenite decomposition during cooling at strain per pass 0.3 after reheating at 1200°C.

During multi-pass deformation process, grain refinement takes place as well as ferrite formation from austenite. Furthermore, incompleteness of recrystallisation after interpass holding means a “retained” strain at the start of the next pass. All these factors have been considered in the current model for deformation force calculation, the evolution of which is shown in Fig. 6. The decrease of stress after strain 4.2 at 760°C corresponds to the formation of a significant amount of ferrite, Fig. 5, as ferrite is a weaker phase than austenite. The deformation force calculation has been carried for a number of steels, Fig. 7-10, with alloy compositions and experimental details given in Table 1 [5,6,7].

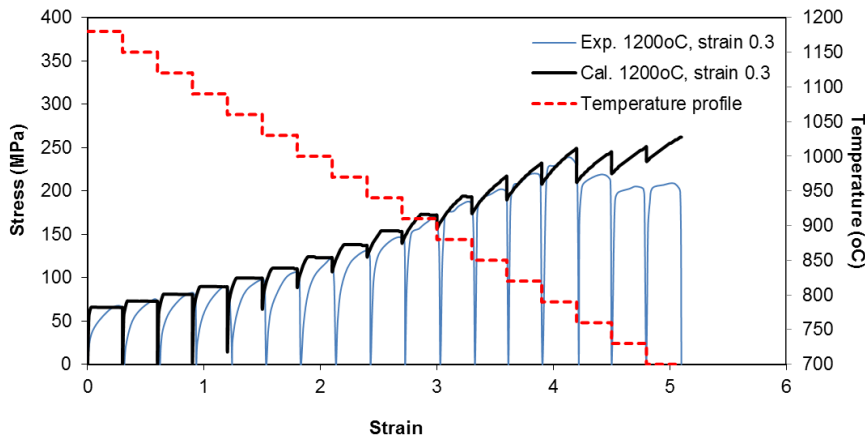


Fig. 6, Evolution of force during deformation at strain per pass 0.3 after reheating at 1200°C.

Table 1. Alloy information and deformation schedule.

Alloy composition (wt%)	Deformation schedule	Ref.
Fe-0.2C-0.2Si-1.0Mn-0.007Nb-0.0056N	Reheating at 1250°C 20 passes, 1 <sup>st</sup> pass at 1150°C, last pass at 675°C Interpass time 20 s, temperature step 25°C Strain rate is 3.63 s <sup>-1</sup> and strain per pass 0.35	Gomez et al. [5]
Fe-0.05C-1.58Mn-0.04Si-0.03Nb-0.16Mn-0.005N	Reheating at 1410-1430°C 20 passes, 1 <sup>st</sup> pass at 1150°C, last pass at 770°C Interpass time 10 s, temperature step 20°C Strain rate is 1.0 s <sup>-1</sup> and strain per pass 0.4	Pereda et al. [6]
Fe-0.05C-0.29Mn-0.15Si-0.025Cu-0.01Ni-0.057Cr-0.006Mn	Reheating at 1280°C 20 passes, 1 <sup>st</sup> pass at 1220°C, last pass at 600°C Interpass time 30 s, temperature step 32.63°C Strain rate is 2.0 s <sup>-1</sup> and strain per pass 0.3	Samuel et al. [7]
Fe-0.07C-0.57Mn-0.18Si-0.027Nb-0.031Cu-0.017Ni-0.024Cr-0.004Mo	Reheating at 1280°C 20 passes, 1 <sup>st</sup> pass at 1260°C, last pass at 760°C Interpass time 30 s, temperature step 26.32°C Strain rate is 2.0 s <sup>-1</sup> and strain per pass 0.3	Samuel et al. [7]

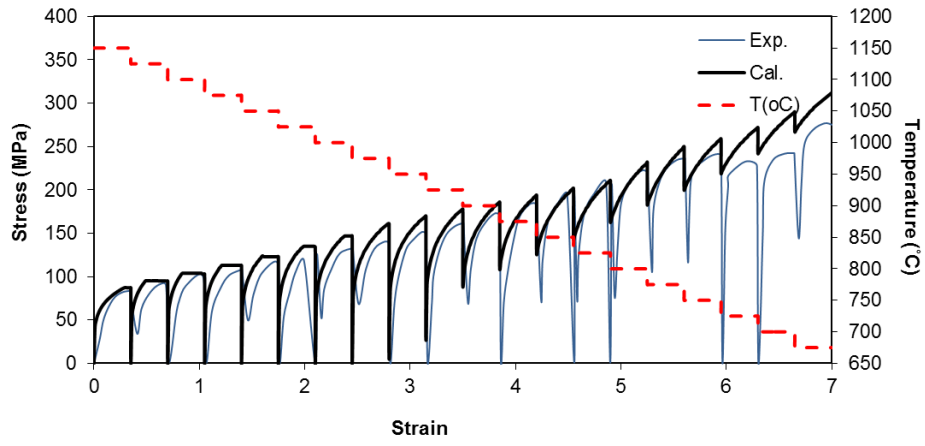


Fig. 7, Evolution of force during deformation of a Nb microalloyed steel (Gomez et al. [5]).

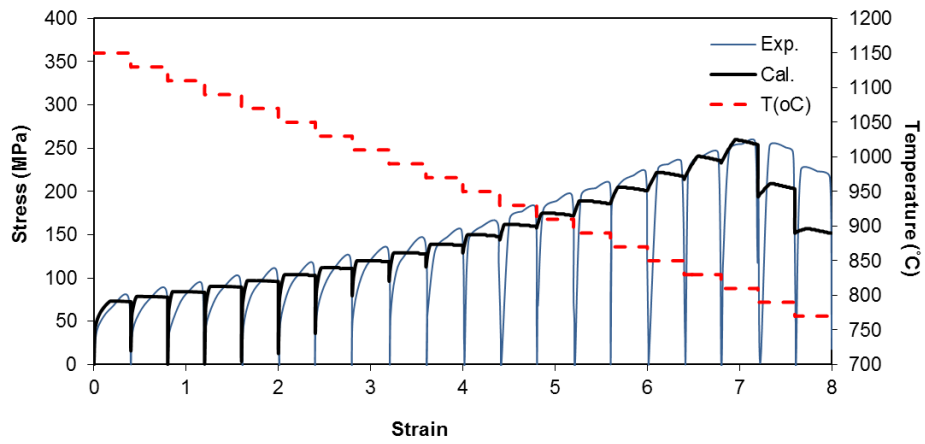


Fig. 8, Evolution of force during deformation of a Nb microalloyed steel (Pereda et al. [6]).

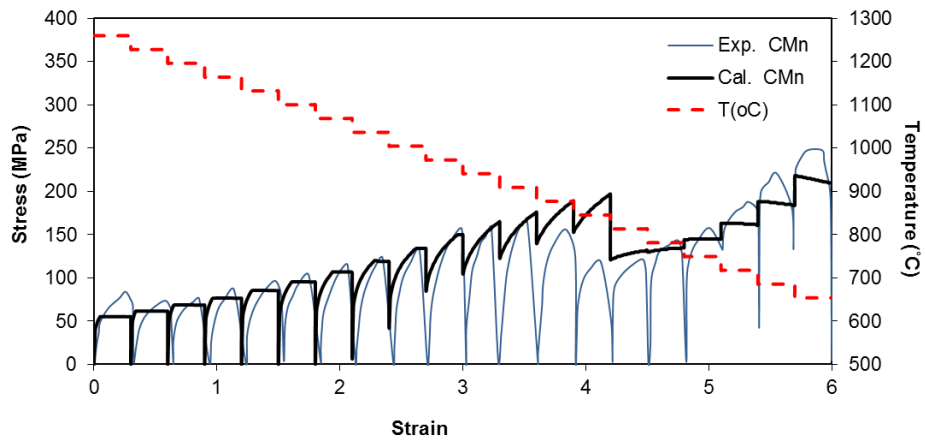


Fig. 9, Evolution of force during deformation of a CMn steel without Nb (Samuel et al. [7]).

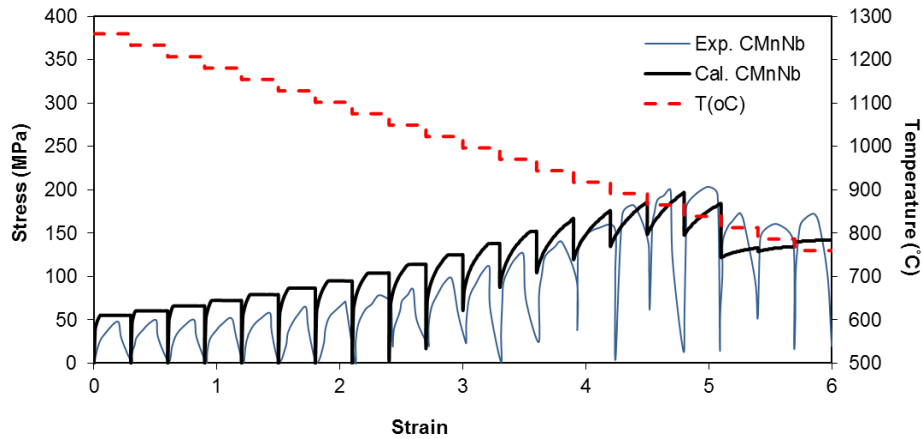


Fig. 10, Evolution of force during deformation of a CMn steel with Nb (Samuel et al. [7]).

In addition to the modelling of microstructural evolution and rolling force during hot rolling, JMatPro can also help in many other aspects of the rolling process (Fig. 1), as described below:

- Reheating

“Step Temperature” calculation can be used to determine the lowest reheating temperature that allows the desired alloying elements to be retained in solid solution. “High Temperature Strength” can be used to calculate the strength at the reheating temperature so as to determine whether the steel is soft enough to be rolled.

- Accelerated cooling and cooling beds

Fig. 5 shows the formation of martensite when cooling after hot deformation is assumed to be at the same rate as that during deformation. In practice, cooling after rolling will be controlled differently so as to achieve desired microstructure. If such a cooling profile is known, one can use the “Quench Properties” calculation to check whether the desired microstructure can be achieved.

## References

1. Z. Guo and A.P. Miodownik, Modelling deformation-induced precipitation kinetics in microalloyed steels during hot rolling, *Materials Science Forum*, 706-709 (2012), 2728-2733.
2. A.I. Fernández, P. Uranga, B. López and J.M. Rodríguez-Ibabe, Static recrystallization behaviour of a wide range of austenite grain sizes in microalloyed steels, *ISIJ International*, 40 (2000), 893-901.
3. R. Abad, A.I. Fernández, B. López and J.M. Rodríguez-Ibabe, Interaction between recrystallization and precipitation during multipass rolling in a low carbon niobium microalloyed steel, *ISIJ International*, 41 (2001), 1373–1382.
4. N. Saunders, Z. Guo, X. Li, A.P. Miodownik and J.P. Schillé, The calculation of TTT and CCT diagrams for general steels, Internal report, Sente Software Ltd.
5. M. Gomez, S.F. Medina and P. Valles, Determination of driving and pinning forces for static recrystallization during hot rolling of a niobium microalloyed steel, *ISIJ International*, 45 (2005), 1711-1720.
6. B. Pereda, B. López and J.M. Rodríguez-Ibabe, Increasing the non-recrystallization temperature of Nb microalloyed steels by Mo addition, in A.J. DeArdo and I.C. Garcia (eds), *Prof. Int. Conf. on Microalloyed Steels*, Warrendale, PA, 2007: AIST, 151-159.
7. F.H. Samuel, S. Yue, J.J. Jonas and B.A. Zbinden, Modeling of flow stress and rolling load of a hot strip mill by torsion testing, *ISIJ International*, 29 (1989), 878-886.